Proceedings of the
Annual Stability Conference
Structural Stability Research Council
Louisville, Kentucky, April 13-16, 2021

Effects of three-dimensional analysis and diaphragm modeling assumptions on seismic collapse of buildings

Gengrui Wei[1], Matthew R. Eatherton[2], Benjamin W. Schafer[3]

Abstract

Two-dimensional (2D) frame analysis has been used extensively to predict the seismic response (e.g., peak story drifts and collapse) of buildings subjected to earthquake excitation. In this type of analysis, the vertical lateral force resisting systems (LFRS) in the building (i.e., braced frames or moment frames) are modeled assuming the horizontal diaphragm system is rigid and that the vertical LFRS responds independent of the rest of the building. In an actual building, the diaphragm system deforms contributing to lateral drifts, and interacts dynamically with the vertical LFRS. Furthermore, inelasticity and failure of the diaphragm can have substantial effect on the seismic behavior and collapse of the overall building. It might be expected, therefore, that 2D frame analysis would result in smaller estimates of seismic collapse potential than three-dimensional (3D) analysis. For this reason, FEMA P695 specifies that the collapse margin ratio obtained from 3D analyses should be amplified by a factor of 1.2, irrespective of diaphragm modeling approach, to account for larger collapse potential found in 3D analyses compared to 2D analyses.

To understand the effects of 3D analysis, different diaphragm modeling assumptions, and unidirectional vs. bidirectional seismic excitation on the seismic collapse response of buildings, a computational study was conducted with models varying in complexity from those equivalent to a nonlinear 2D frame analysis to a full 3D building analysis with nonlinear behavior in both the vertical LFRS and the diaphragm system. Buckling restrained braced frames were used as the vertical LFRS and the diaphragm system was concrete-filled steel deck at the floors and bare steel deck at the roof. Beams and columns were modeled using nonlinear beam-column elements, while the diaphragm was modeled as a system of diagonal truss elements that were either rigid, elastic, or nonlinear. Nonlinear response history analyses were performed with the far field ground motion set from FEMA P695 and resulting performance in terms of drifts and collapse were evaluated.

Results showed that diaphragm elasticity led to an increase in the period for the first four modes of between 5% and 34%. Diaphragm deformations led to similar collapse probabilities, but as much as 20% larger story drift for the design earthquake and maximum considered earthquake hazard levels. However, when the hazard level was increased to a level called the $ACMR_{10\%}$ in FEMA P695, the building behavior changed and diaphragm inelasticity shared some of the displacement demands, thereby reducing the deformation demands in the BRBF and preventing some of the collapses associated with BRB fracture. At this larger hazard level, the building models that included diaphragm inelasticity had up to 43% fewer collapses than those with rigid

[1] Graduate Research Assistant, Virginia Tech, <gwei1@vt.edu>
[2] Associate Professor, Virginia Tech, <meather@vt.edu >
[3] Professor, Johns Hopkins University, <schafer@jhu.edu>

or elastic diaphragms. It was also found that subjecting the models to bidirectional ground motion pairs as compared to single unidirectional ground motions, led to 11% to 16% larger peak in-plane BRBF drift demands at the MCE hazard level, and as much as 80% more collapses at the $ACMR_{10\%}$ hazard level. This implies that the FEMA P695 factor of 1.2 on collapse margin ratio for 3D models subjected to bidirectional ground motion pairs may warrant additional investigation

1. Introduction

The seismic behavior and performance of a building depend on both the vertical lateral force resisting system (LFRS), such as braced frames, and the horizontal LFRS, such as the roof and floor diaphragms. During an earthquake, lateral inertial forces are transferred through the diaphragms to the vertical portions of the LFRS. Historically, seismic design of buildings assumes that the vertical elements of the LFRS control the dynamics of the building (e.g. periods and mode shapes) and that the vertical LFRS is the primary source of inelastic actions and hysteretic energy dissipation in the structure. In conjunction with this assumption, two-dimensional (2D) frame analysis has been widely used in the design and analysis of buildings (Krawinkler, 2000; Zareian et al., 2010; Farahi and Mofdi, 2013; Elkady and Lignos 2014; Malakoutian et al., 2015). Implicit assumptions made when using 2D frame analysis, are that the diaphragm system is rigid, the diaphragm dissipates no seismic energy, and the building does not experience torsion. In other words, 2D frame analysis assumes that the vertical LFRS responds independent of the rest of the building. However, real-world building structures behave as a 3D system during earthquakes, and the elastic and inelastic deformations of the diaphragm will interact with the deformations in the vertical LFRS and affect the seismic behavior and performance of the building.

A useful tool in evaluating seismic collapse performance of buildings is FEMA P695 (FEMA, 2009) which provides a methodology for assessing whether a seismic design approach provides sufficient protection against collapse. In that methodology, the collapse margin ratio (CMR) is introduced to quantify the safety margin of structures against collapse. Per FEMA P695, when three-dimensional (3D) models are used for response history analysis, the obtained collapse margin ratio should be amplified by a factor of 1.2 to account for larger collapse potential found in 3D analysis compared to 2D analysis. However, FEMA P695 does not provide quantitative justifications for the 1.2 factor, and this factor is also not tied to how the diaphragm is modeled (e.g., rigid, semi-rigid, or nonlinear). Furthermore, there is little data in the literature about how 3D analysis, diaphragm modeling approaches, and bidirectional loading affect seismic collapse (Koliou et al., 2016; Leng et al., 2020).

A computational study was performed to understand the effects of (1) 3D analysis vs. 2D analysis, (2) diaphragm modeling as rigid, elastic, or nonlinear, and (3) bidirectional vs. unidirectional application of ground motions on the seismic collapse response of a building. The models vary in complexity from those equivalent to a nonlinear 2D frame analysis to a full 3D building analysis with nonlinear behavior in both the vertical LFRS and the diaphragm system. Nonlinear beam-column elements were used to model the buckling restrained braced frames and nonlinear truss elements were used in the horizontal planes to capture the concrete-filled steel deck diaphragms at the floors and bare steel deck diaphragm at the roof. A suite of nonlinear response history analyses was conducted with ground motions scaled to different hazard levels.

2. Details of Building Models

The eight-story building archetype from Torabian et al. (2019) was adopted for use in this study. This section provides some details of the archetype building and the modeling schemes.

2.1 Archetype Building

The eight-story building archetype was designed to the current U.S. building code including ASCE 7-16 (ASCE, 2016), AISC 341-16 (AISC, 2016a), and AISC 360-16 (AISC, 2016b). The building is assumed to be located at an arbitrary site in Irvine, California, with risk category II and site class D. The design spectral accelerations at short periods and at a 1-second period are 1.030g and 0.569g, respectively. Fig. 1 shows a typical floor plan of the building with a dimension of 300 *ft* by 100 *ft* and a story height of 14 *ft* at the first story and 12.5 *ft* for all upper stories. Buckling-restrained braced frames (BRBFs) with elevations shown in Fig. 2, are located in two perimeter bays on all four sides of the building. A dead load of 42 *psf* and a live load of 20 *psf* were considered for the roof, whereas dead load of 85 *psf* and live load of 50 *psf* were used for the floors. The diaphragms were designed based on conventional ELF-based diaphragm demands per ASCE 7-16. Additional details for the design of the building archetype can be found in Torabian et al (2019) and Wei et al. (2020).

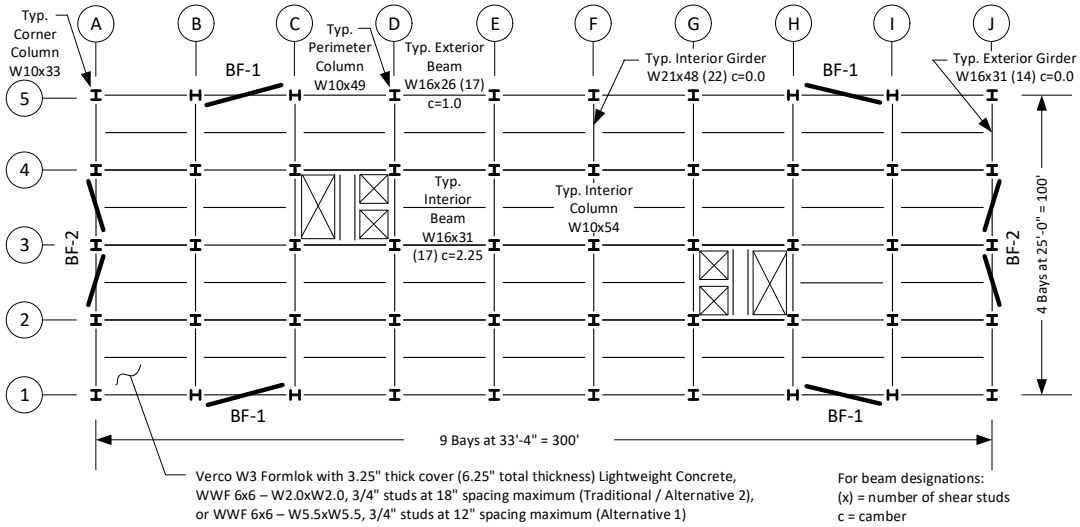

Figure 1: Typical floor plan of building archetype

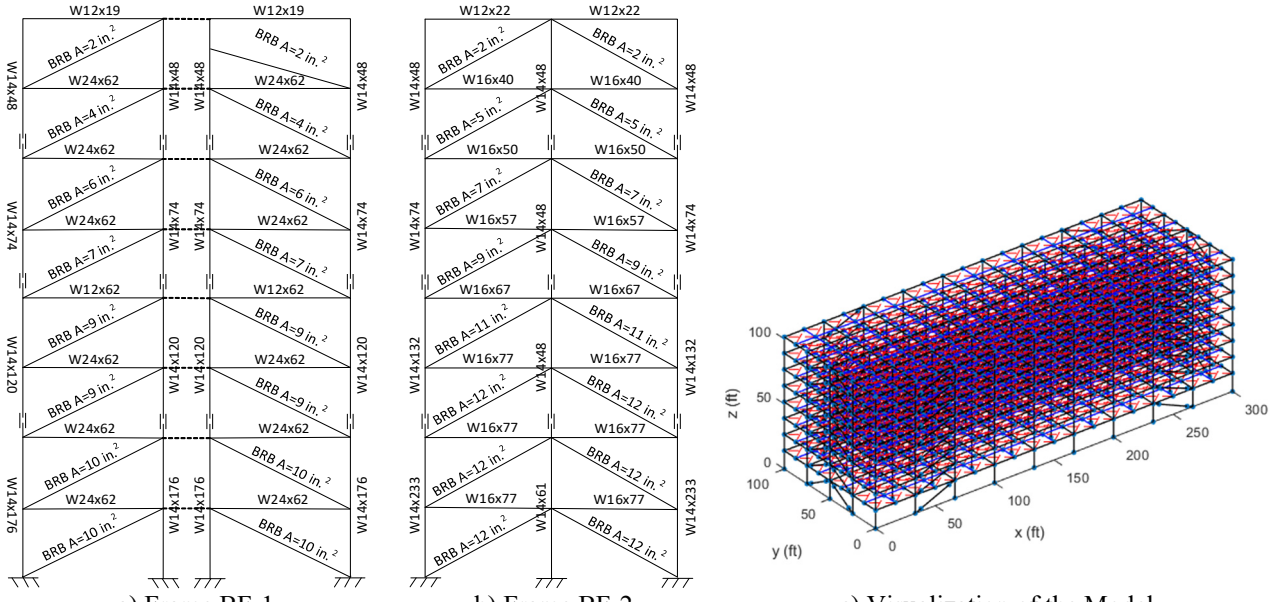

a) Frame BF-1 b) Frame BF-2 c) Visualization of the Model

Figure 2: Typical BRBF elevations

2.2 Overview of Computational Model and Modeling Schemes

The computational models were created using the software, *OpenSees* (Mazzoni et al, 2006), with all columns pinned at their base, and pinned connections at all beam-to-column and beam-to-beam joints with the exception of the braced bays which use rigid connections at the beam-to-column joint to simulate the influences of the gusset plates. Columns and beams were represented by nonlinear force-based beam-column elements with fiber-section formulation and linear kinematic hardening material with a yield stress equal to 60 ksi, elastic modulus equal to 29,000 ksi, shear modulus equal to 11,500 ksi, and hardening modulus equal to 450 ksi. The fiber section is formulated with eight Gauss-Lobatto integration points along the element, and the number of fibers along the web depth, web thickness, flange width, and flange thickness of the cross section is 16, 2, 16, and 4, respectively. Geometric nonlinearity was considered by including the gravity loads and using the P-Delta coordinate transformation algorithm in *OpenSees* for the columns. Per FEMA P695, the gravity loads include a combination of dead and live loads ($1.05D+0.25L$). Mass was determined from the dead loads ($m=D/g$) and lumped at the column nodes on each floor. Rayleigh damping with a critical damping ratio equal to 2% for the 1st and 4th mode was used for the building models. P-Delta effects were captured explicitly by the application of gravity loads and geometric nonlinearity in the model.

Nonlinear response history analyses were performed with the building model subjected to the suite of 44 FEMA P695 far-field earthquake motions scaled to three different hazard levels: 1) Design Earthquake (DE); 2) Maximum Considered Earthquake (MCE) and 3) A scale level based on adjusted collapse marginal ratio ($ACMR_{10\%}$), with scale factors of 1.67, 2.50, and 2.86, respectively. The scale factor for the DE hazard level was determined using the scaling approach and Seismic Design Category D_{max} from FEMA P695. The spectral accelerations associated with D_{max} are similar to the design spectral accelerations used to design the archetype building. The MCE scale factor was then taken as the DE scale factor multiplied by 3/2. The third scale factor is used to determine collapse acceptability (i.e., if less than 50% of the ground motions cause collapse then the design is acceptable) and was obtained as described in Appendix F.3 of FEMA P695. First an acceptable value of adjusted collapse margin ratio ($ACMR_{10\%}$) is obtained with assumed total system collapse uncertainty. Then, the period-based ductility (μ_T) is obtained from the pushover analysis and the spectral shape factor (*SSF*) and collapse margin ratio (*CMR*) are obtained. Finally, the scale factor based on $ACMR_{10\%}$ is obtained by multiplying the collapse margin ratio by the scale factor for MCE. The scale factors were determined based on the properties of the building with inelastic diaphragms and the same scale factors were applied to all building models described in this paper.

A total of nine building models were considered, including every combination of three diaphragm modeling assumptions (i.e., rigid, elastic, and inelastic diaphragms), and three earthquake loading patterns (i.e., bidirectional loading, unidirectional loading in the longitudinal (x) direction, and unidirectional loading in the transvers (y) direction). For simplicity, they are herein referred to as: "RigidBi", "RigidUniX", "RigidUniY", "ElasticBi", "ElasticUniX", "ElasticUniY", "InelasticBi", "InelasticUniX" and "InelasticUniY". The prefix describes the approach to diaphragm modeling and the suffix refers to the ground motion direction.

2.3 Diaphragm Modeling

The roof and floors of the archetype building were designed as bare steel deck and concrete-filled steel deck diaphragms, respectively. Existing cantilever diaphragm tests as depicted in Fig. 3a were

used to calibrate nonlinear hysteretic models for the in-plane diaphragm response of the models with the inelastic diaphragm modeling assumption. For the bare steel deck roof diaphragm, Specimen 33 of Martin (2002) with 20-gage 1.5 *in*. deep B-deck and employing PAFs for the structural connectors and screws for the sidelap connections, was used because it had sufficient design strength to match the roof demands. For the concrete-filled steel deck diaphragm, test specimen 3/6.25-4-L-NF-DT from Avellaneda et al. (2019) was used, which consisted of 3 *in*. deck, with lightweight concrete fill and 6.25 *in*. total thickness. These specimens are referred to here as SP1 and SP2, respectively. Nonlinear truss elements with the Pinching4 material model in *OpenSees*, as depicted in Fig. 3b, were used to simulate the in-plane diaphragm response. Table 1 provides the final calibrated Pinching4 material parameters including backbone stresses and strains and cyclic strength and stiffness degradation for the two selected diaphragm specimens. A comparison of the hysteretic response from the calibrated diaphragm simulation and that from the experiment is shown in Fig. 4. A scale factor of 0.91 and 1.19 was used to scale the Pinching4 backbone strength to match the design demands of the roof and floor diaphragms, respectively.

The models with the elastic and rigid diaphragm assumption are identical to the models with inelastic diaphragms except that elastic material was used for the diaphragm truss elements instead of the Pinching4 material model. The stiffness of the elastic material for models with elastic diaphragms is equal to the initial stiffness of the Pinching4 material model. This stiffness is amplified by a factor of 1000 for the elastic material of rigid diaphragms.

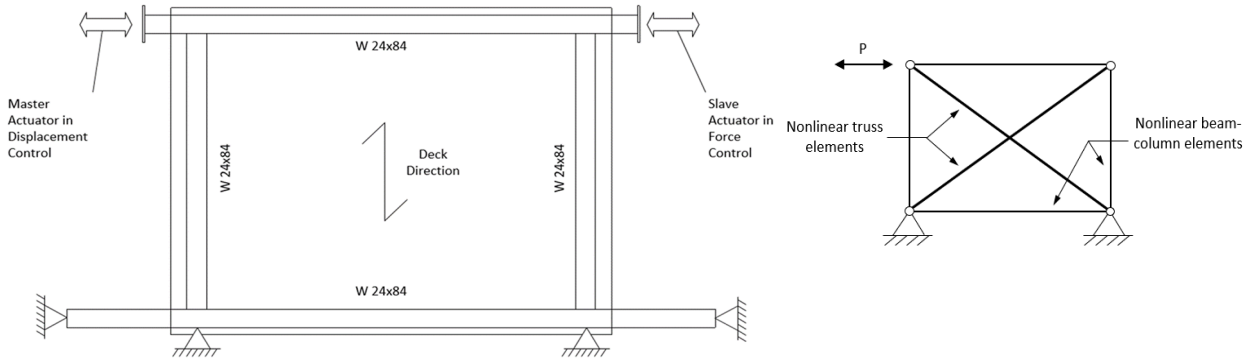

(a) (b)

Figure 3: Cantilever diaphragm test: (a) schematic view of SP2 test setup, (b) computational model

Table 1: Calibrated Pinching4 Material Model Parameters

Test	Backbone				Pinching			Strength Degradation					Stiffness Degradation					Energy Dissipation
	ε_1, σ_1 (ksi)	ε_2, σ_2 (ksi)	ε_3, σ_3 (ksi)	ε_4, σ_4 (ksi)	r_{Δ^+}, r_{Δ^-}	r_{F^+}, r_{F^-}	u_{F^+}, u_{F^-}	gF_1	gF_2	gF_3	gF_4	gF_{lim}	gK_1, gD_1	gK_2, gD_2	gK_3, gD_3	gK_4, gD_4	gK_{lim}, gD_{lim}	gE
SP1	0.0008, 22.18	0.0017, 28.90	0.0033, 30.69	0.0053, 23.97	0.20, 0.35	0.20, 0.35	0.10, 0.12	0	0.35	0	0.70	0.90	0, 0	0, 0.50	0, 0	0, 0.75	0, 0.90	4.31
SP2	0.0005, 63.46	0.0006, 76.41	0.0014, 107.40	0.0143, 48.33	-0.06, -0.06	0.12, 0.12	0.11, 0.11	0	0.83	0	0.46	0.33	1.09, 0.14	0.76, 0.47	0.32, 0.12	0.75, 0.10	1.04, 0.61	4.29

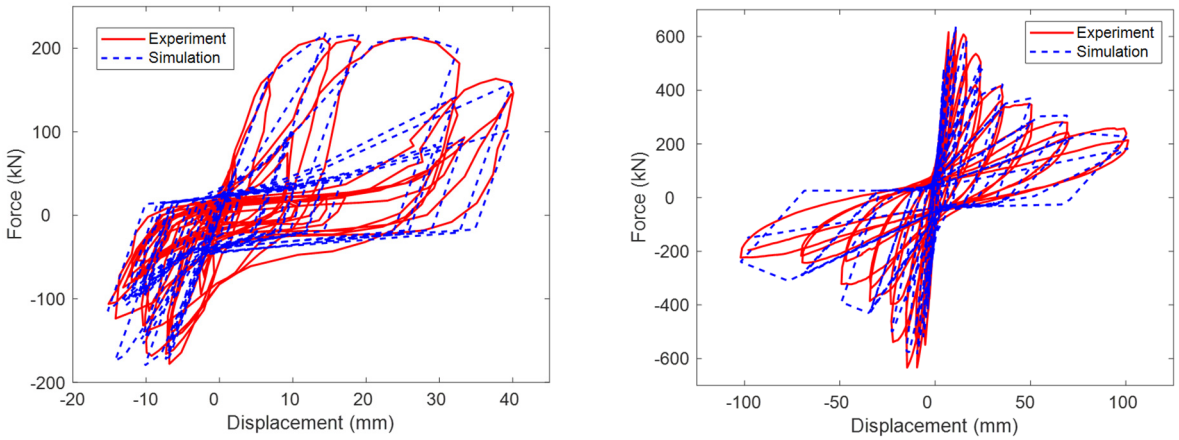

(a) (b)

Figure 4: Hysteretic response of diaphragm from experiment and simulation: (a) SP1, (b) SP2

2.4 Brace Modeling

As shown in Fig. 5a, the BRB core (restrained yielding segment) is modeled by a nonlinear truss element with Steel4 material model in *OpenSees*. The non-yielding segments on both ends are modeled with elastic beam-column elements, and another elastic beam-column element with negligible cross-sectional area and large bending stiffness is also used to connect the non-yielding segments to fix the rotational degrees of freedom and prevent instability of the truss element. The BRB core material model parameters were calibrated to match BRB tests presented in Newell et al. (2006). Fig. 5b shows an example for the hysteretic curves of the calibrated model as compared to the test results and calibrated Steel4 material parameters are provided in Table 3.

A fatigue material model called "uniaxialMaterial Fatigue" in *OpenSees* was used to capture BRB fracture based on two parameters: ε_0, the value of strain at which one cycle will cause failure, and m, the slope of Coffin-Manson (Coffin, 1954; Manson, 1954) curve in log-log space. The value of ε_0 was taken as 0.2 based on the elongation of A36 core steel material per ASTM standards (ASTM, 2019). A value of $m = 0.5976$ was found to produce fracture consistent with the only test by Newell et al. (2006) that experienced fracture, as demonstrated in Fig. 5b.

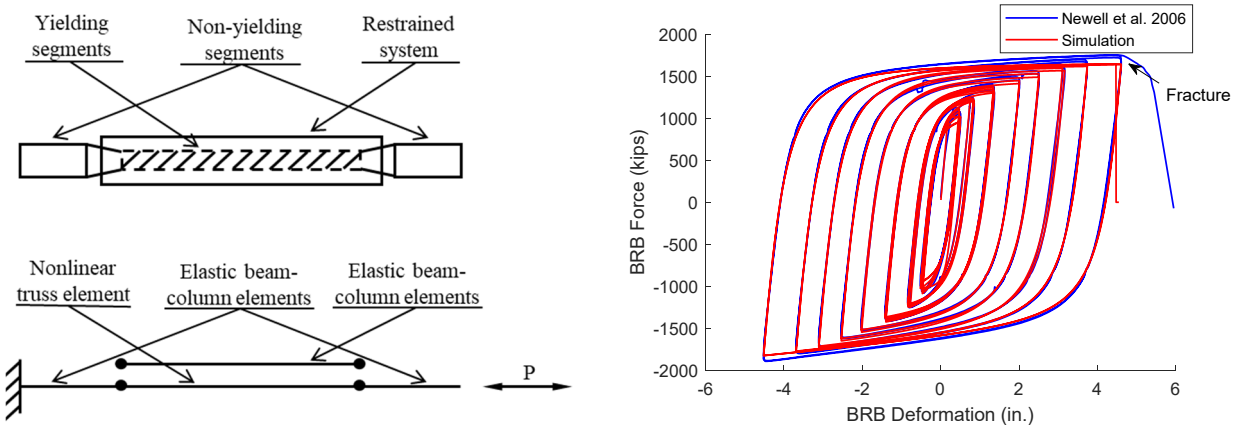

(a) Computational model (b) Calibration of BRB Steel4 material model

Figure 5: Configuration of BRB computational model and example hysteretic curve for BRB Steel4 calibration

Table 3: Calibrated Steel4 Parameters for BRB model

b_k	R_0	r_1	r_2	b_i	b_l	ρ_i	R_i	l_{yp}	f_u	R_u
0	20.9837	0.9122	0.1209	0.0306	0	0.7262	1.3134	18.2022	70.3000	620.6286
b_{kc}	R_{0c}	r_{1c}	r_{2c}	b_{ic}	b_{lc}	ρ_{ic}	R_{ic}	l_{ypc}	f_{uc}	R_{uc}
0.0121	18.9116	0.9133	0.1232	0.0020	0	0.9061	2.9727	37.3548	108.4701	583.5268

3. Analysis Results

Details and discussion of the analysis results are presented in this section.

3.1 Eigenvalue Analyses

To study the effect of diaphragm rigidity on the modal properties of the building structure, eigenvalue analysis was performed for the building models with rigid and elastic diaphragms to obtain their mode shapes and periods. It is noted that the mode shapes and periods for the models with elastic and inelastic diaphragms are identical because they possess the same initial stiffness. Fig. 6 shows the mode shapes for the first four modes, wherein diaphragm deformations are shown to be small relative to the BRBF deformations for the first three modes which represent the fundamental modes for x-axis motion, y-axis motion, and torsion, respectively. However, for the fourth mode which represents a higher mode of deformation for y-axis motion, the diaphragm deformations account for a more significant portion of the total displacements. Table 4 provides the first four periods of the building models obtained from the eigenvalue analysis. It is observed that diaphragm deflections increased the modal periods by between 5% and 34% and that increasing periods can result in decreasing spectral accelerations for a typical ground motion response spectrum.

1st mode

2nd mode

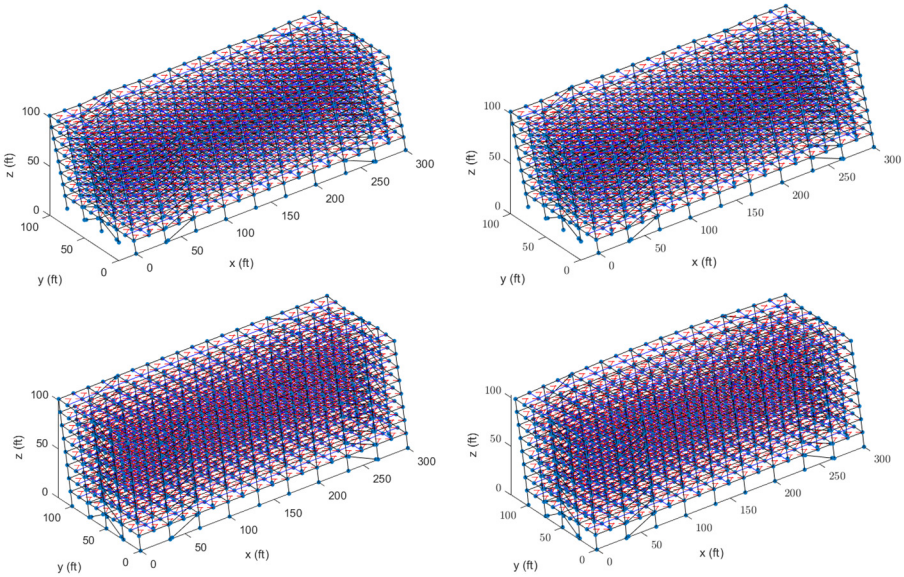

(a) Rigid diapgragm (b) Elastic/inelastic diaphragm

Figure 6: Mode shapes of building models with rigid and elastic/inelastic diaphragm

3rd mode

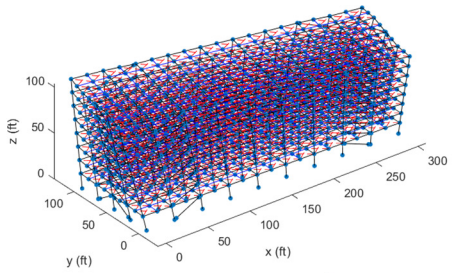

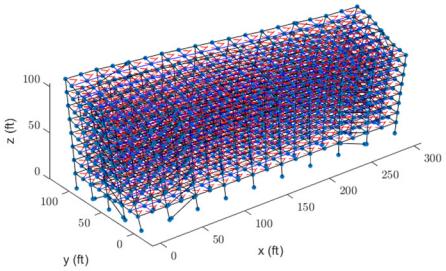

4th mode

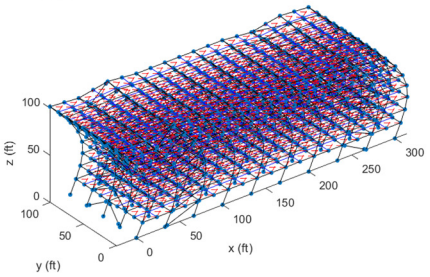

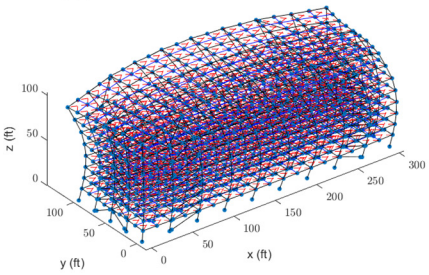

(a) Rigid diapgragm (b) Elastic/inelastic diaphragm

Figure 6 (Continued): Mode shapes of building models with rigid and elastic/inelastic diaphragm

Table 4: Periods of building models with rigid and elastic/inelastic diaphragm

Mode	Periods (sec)		
	Rigid Diaphragm	Elastic/Inelastic Diaphragm	Difference
1st mode	1.95	2.06	6%
2nd mode	1.66	1.83	10%
3rd mode	1.03	1.08	5%
4th mode	0.72	0.96	34%

3.2 Nonlinear Response History Analyses

The results of the response history analyses are presented in the following order: 1) evaluating median peak story drifts for all models, 2) examining response to one ground motion to help understand behavior, 3) investigating collapse results, and 4) discussion of the effect of bidirectional vs. unidirectional ground motions.

Fig.7 shows the distribution of median peak story drift ratio (SDR) in the y direction (short dimension of the building) along the building height for the building models subjected to bidirectional earthquake loading at all three hazard levels. Two different story drifts are plotted, i.e., the median peak story drift for the BRBFs and the median peak total story drift of the building which includes the deformation of the BRBFs and the diaphragms. Only one line is plotted for the models with rigid diaphragms because the two are identical.

For the DE and MCE hazard levels, Fig. 7a and 7b show that the peak total story drifts generally get larger as the diaphragm model goes from rigid (RD) to elastic (ED) to inelastic (ID). For lower hazard levels, explicitly modeling diaphragm deformations will increase the total story drifts because the diaphragm is adding flexibility. The added flexibility is demonstrated by the fact that the BRBF story drifts at the DE and MCE levels are quite similar regardless of the diaphragm modeling approach, and that diaphragm deformations act as merely superimposing additional deflections leading to larger total story drift. This is particularly true for smaller motions where the LFRS and diaphragm remain in the elastic range or experience moderate inelasticity. It is also

observed that the story drift at the top story is most affected by the diaphragm modeling assumption because the bare steel deck roof diaphragm is considerably more flexible than the concrete-filled steel deck floor diaphragms.

At the $ACMR_{10\%}$ hazard level, however, the behavior is substantially different as the building models approach collapse. Fig.7c shows that the building models with rigid (RD) and elastic (ED) diaphragms experience median peak story drifts that are approximately two times larger than the model with inelastic diaphragms (ID). To understand why the trend at $ACMR_{10\%}$ hazard level is opposite that at the lower hazard levels, it is necessary to examine all the possible reasons that changing the diaphragm model affects peak drifts:

1. Diaphragm deflections add flexibility to the structure which increase total story drift for ED and ID.
2. The mode shapes, particularly the fourth mode in Fig. 6 has large diaphragm deformation component that could increase upper story drifts for ED and ID.
3. The periods for models with ED and ID are larger than RD and thus the associated spectral accelerations and peak drifts would be expected to decrease for ED and ID.
4. Inelastic action of the diaphragm would dissipate seismic energy such that peak drifts are decreased for ID.
5. Inelastic deformations in the diaphragm reduce the deformation demands in the BRBF which can greatly decrease peak drifts in ID, especially as the BRBs near fracture.

For the DE and MCE hazard levels, reasons (1) and (2) lead to as much as 20% increase in story drifts for the models with elastic and inelastic diaphragms as compared to the rigid diaphragm models. At the $ACMR_{10\%}$ hazard level, reason (5) creates substantially smaller story drifts in the ID models as demonstrated by the following discussion of a single ground motion run.

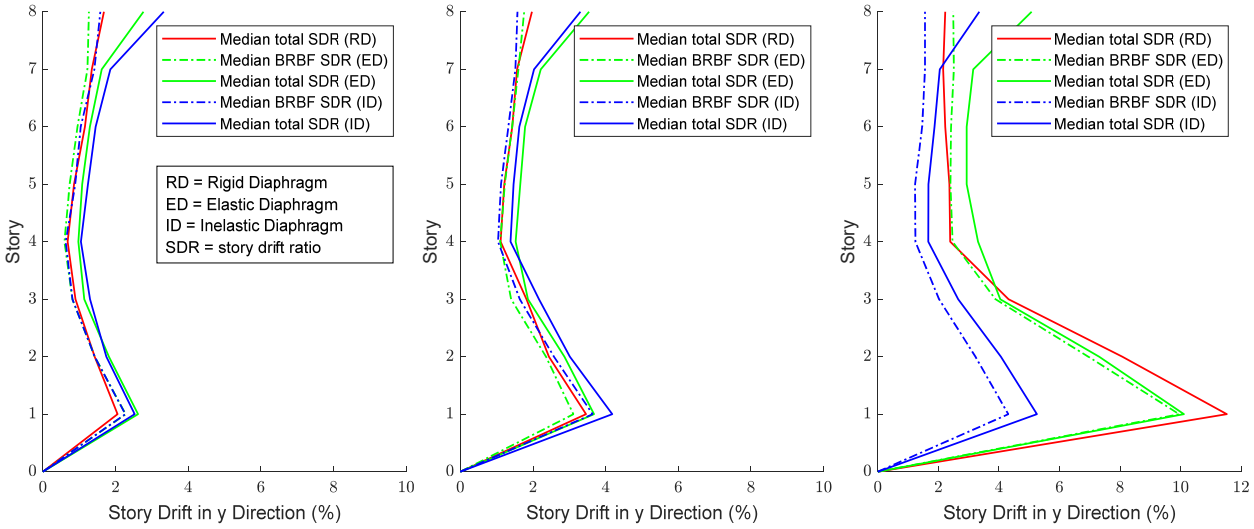

(a) DE (b) MCE (c) $ACMR_{10\%}$

Figure 7: Distribution of median peak story drift in y direction along building height with different diaphragm modeling assumption and bidirectional earthquake loading

The responses of the rigid diaphragm (RD) and inelastic diaphragm (ID) building models subjected to bidirectional ground motion from the Nishi-Akashi recording station during the 1995 Kobe

Earthquake scaled to $ACMR_{10\%}$ are shown in Fig. 8. Fig 8a shows the resultant story drift (i.e., square root of the sum of the squares of the story drift ratios in the x and y directions) for the first story and Fig. 8b shows the BRB core strain for one of the BRBs in the first story along the x-axis. During the first 10 seconds of the motion, the two building models experienced similar story drift, but the BRB core strain was larger for the RD case. In a context where earthquake motions are considered as applying a displacement demand on the structure, this result can be interpreted as follows: making the diaphragm rigid, forces more deformation demand into the BRBF. Between 10 seconds and 25 seconds, the BRB undergoes a ratcheting behavior as the story drift goes from approximately 5% to more than 10%. The P-Δ effect contributes to this ratcheting behavior as does the low hardening slope of the BRBs (Kiggins and Uang 2006). After 25 seconds, the damage index associated with the Fatigue fracture law used in the model reaches a value of 1.0 which causes the BRB strength to go to zero and story drift to increase toward simulated collapse.

Viewed another way, the first 8 seconds of the ground motion may represent building behavior during ground motions such as the DE and MCE hazard level where the inelastic diaphragm model experiences large story drift. The latter part of the ground motion represents building behavior at $ACMR_{10\%}$ and near collapse where the rigid diaphragm model forces larger deformation demands into the BRBF which leads to BRB fracture and collapse. At the $ACMR_{10\%}$ hazard level, the number of ground motions resulting in BRB fracture was found to be 8, 20, and 21 for the building models with inelastic, elastic, and rigid diaphragms, respectively.

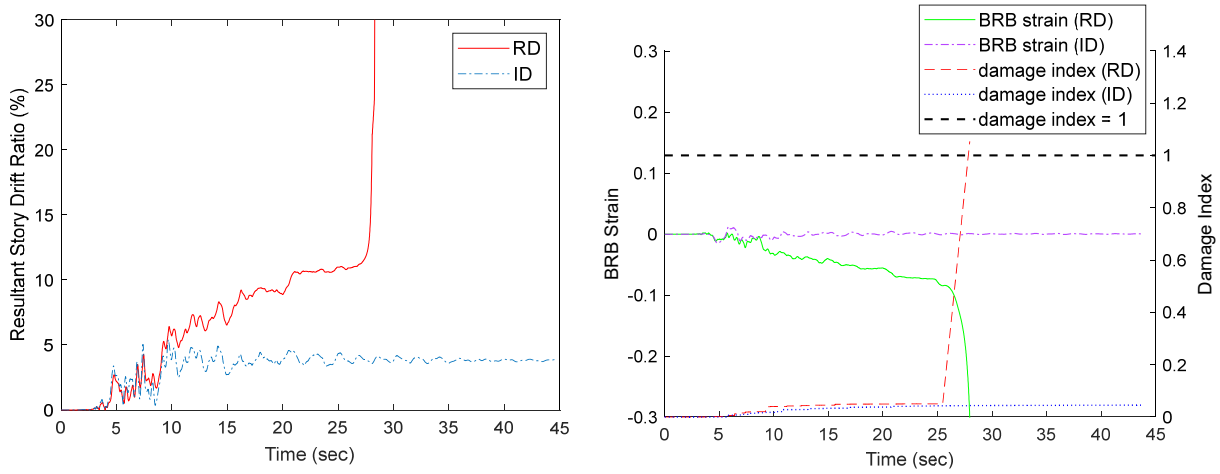

(a) Story drift (b) BRB Behavior

Figure 8: Building response with rigid and inelastic diaphragms subjected to $ACMR_{10\%}$ hazard level and bidirectional ground motions for the Nishi-Akashi motion of 1995 Kobe, Japan earthquake

To investigate the seismic collapse performance of the buildings with different diaphragm modeling assumptions and earthquake loading patterns, the number of ground motions causing collapse was tabulated for each hazard level. Three criteria were considered for the definition of building collapse: 1) maximum story drift ratio exceeds 10%; 2) maximum diaphragm shear angle exceeds 4% - this limit is determined based on the evaluation of past cantilever diaphragm tests and shear connector tests; and 3) convergence failure occurs in the analysis – if the first two criteria were not triggered, these were evaluated on a case-by-case basis (see Wei et al. 2020 for more details).

Table 5 provides the percent of ground motions causing collapse for building models subjected to bidirectional ground motions. For the DE and MCE hazard levels, it is observed that the number of ground motions causing collapse was similar regardless of how the diaphragm was modelled. However, at the $ACMR_{10\%}$ hazard level, the model with rigid diaphragm had almost twice as many ground motions causing collapse at the model with inelastic diaphragm. Since simulated collapse in these building models is sensitive to large BRB core strains which cause ratcheting in the story drift response and BRB fracture, models that forced more deformation demand into the BRBF (i.e., rigid diaphragm models), result in substantially more collapses.

Table 5: Proportion of ground motions causing collapse for models subjected to bidirectional motions.

Diaphragm Rigidity	Hazard Level		
	DE	MCE	$ACMR_{10\%}$
Rigid	4.5%	25.0%	64.3%
Elastic	4.5%	20.5%	54.8%
Inelastic	4.5%	25.0%	36.4%

The effect of bidirectional ground motions compared to unidirectional ground motions is also evaluated. Fig. 9 shows the median peak story drifts of the building models with rigid diaphragms subjected to unidirectional and bidirectional earthquake loading at the MCE hazard level. It can be observed from Fig. 9a that the median peak x-direction story drift in the first story BRBF increases by 11% when the loading is changed from single ground motions applied in the x-direction only to bidirectional ground motion pairs. Similarly, Fig. 9b shows a 16% increase in first story BRBF drift demand with bidirectional ground motions. This shows that the application of bidirectional ground motion pairs leads to larger in-plane drift demands in the braced frames than unidirectional ground motions, especially at stories subjected to large drift where P-Delta effects are more significant. Fig. 9c shows the expected result that the peak resultant drifts (i.e., along the diagonal), are larger with the application of ground motion pairs. This result, however does not directly relate to the story drift demands on the BRBF in the X and Y direction like Fig. 9a and 9b.

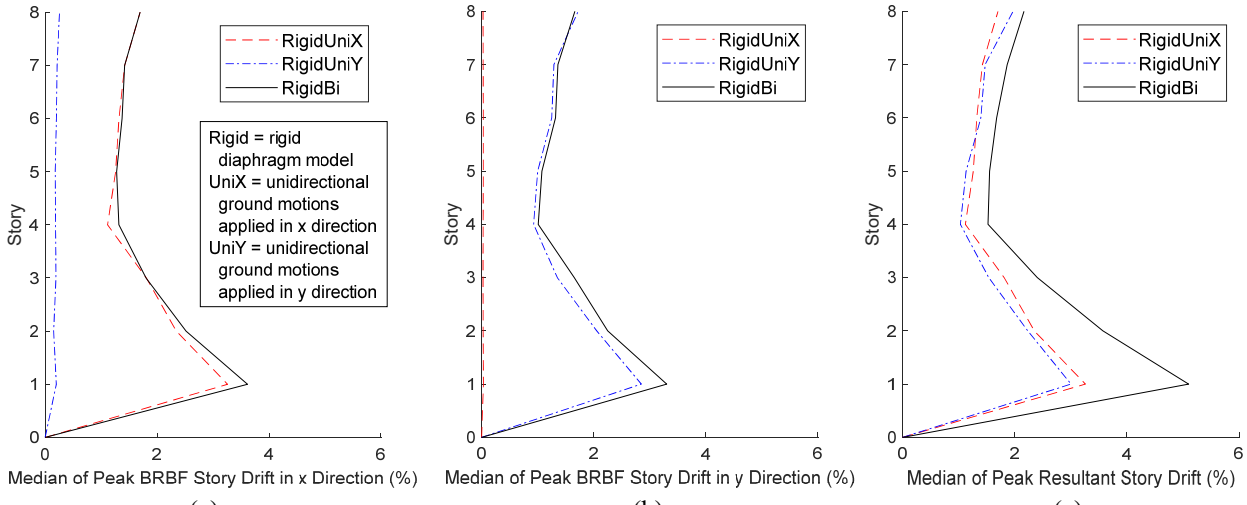

(a) (b) (c)

Figure 9: Distribution of median peak story drifts along building height for building models with rigid diaphragms considering unidirectional and bidirectional earthquake loading at MCE hazard level

Table 6 provides the ratio of ground motions causing building collapse for all building models analyzed and separated for unidirectional and bidirectional earthquake loading. The likelihood of collapse was significantly larger with bidirectional ground motions for both the rigid diaphragm and elastic diaphragm models. This indicates that the probability of building collapse can be underestimated using 2D building models subjected to unidirectional earthquake loading. FEMA P695 accounts for this difference by applying a factor of 1.2 to the collapse margin ratio obtained from 3D building models subjected to bidirectional ground motions. The ratios of the number of ground motions causing collapse using unidirectional X or Y direction motions to the number of ground motions causing collapse when subjected to bidirectional motions are given in the last two columns of Table 6 for the $ACMR_{10\%}$ hazard level. These results are not tabulated for other hazard levels because they represent the tail of the collapse distribution and thus are not as easy to quantify with 44 motions. Table 6 shows that the number of ground motions that cause collapse for the rigid and elastic diaphragm building models was between 1.3 and 1.8 times larger when bidirectional ground motions are used. While this ratio on number of ground motions causing collapse is not directly comparable to the 1.2 factor on collapse margin ratio in FEMA P695, it suggests that the factor may warrant additional investigation. The models with inelastic diaphragms had a different result in that collapse probabilities were similar regardless of whether the ground motions were applied in one direction or bidirectional.

Table 6: Proportion of ground motions causing collapse for all models

Diaphragm Model	Hazard Level	Earthquake Loading			Ratio	
		X-Direction	Y-Direction	Bi-Directional	Bi / X	Bi / Y
Rigid	DE	2.3%	0.0%	4.5%	-	-
	MCE	13.6%	5.0%	25.0%	-	-
	$ACMR_{10\%}$	48.8%	36.4%	64.3%	1.32	1.77
Elastic	DE	2.3%	0.0%	4.5%	-	-
	MCE	15.9%	6.8%	20.5%	-	-
	$ACMR_{10\%}$	40.5%	30.0%	54.8%	1.35	1.83
Inelastic	DE	4.5%	2.4%	4.5%	-	-
	MCE	16.7%	8.1%	25.0%	-	-
	$ACMR_{10\%}$	40.9%	35.7%	36.4%	0.89	1.02

4. Conclusions

Conventional seismic performance evaluation of steel braced frame buildings primarily focuses on 2D frame analysis where the inelasticity in the diaphragms and its interaction with the inelasticity in the vertical lateral force resisting system are neglected. To investigate the effect of diaphragm modeling assumptions and earthquake loading patterns in 3D collapse modeling of building structures, a series of 8-story building models with buckling restrained braced frames and steel deck diaphragm systems designed to the current US seismic provisions were developed and analyzed with varying diaphragm rigidity (rigid, elastic, or inelastic) and earthquake loading pattern (bidirectional or unidirectional).

Eigenvalue analyses showed that elastic diaphragm deformations participated in the mode shapes and that diaphragm elasticity caused the modal periods to increase by 5% to 34% for the first four modes. Larger building periods that are beyond the peak of the response spectrum are often associated with smaller spectral accelerations.

For the DE and MCE hazard levels, the response history analyses showed that even though the number of ground motions causing building collapse was similar regardless of how the diaphragm was modelled, diaphragm deformations contributed to as much as 20% larger drifts in the models with elastic and inelastic diaphragms as compared to the rigid diaphragms. However, at the $ACMR_{10\%}$ hazard level, inelastic deformations in the diaphragm reduce the deformation demands in the BRBF as the BRBs near fracture, which results in substantially smaller story drifts and up to 43% fewer collapses in buildings with inelastic diaphragms than those with rigid or elastic diaphragms.

For rigid diaphragm building models, it was found that the in-plane BRBF story drift demands were between 11% and 16% larger when the building was subjected to bidirectional ground motion pairs as opposed to single unidirectional ground motions. The number of ground motions that caused collapse of the rigid diaphragm and elastic diaphragm buildings was also notably larger (between 30% and 80% larger) when ground motion pairs, scaled to the $ACMR_{10\%}$ hazard level, were applied compared to unidirectional ground motions. This discrepancy in collapses indicates that the probability of building collapse can be underestimated using 2D building models subjected to unidirectional earthquake loading and the magnitude of the discrepancy implies that the FEMA P695 3D factor of 1.2 on collapse margin ratio may warrant additional investigation

Acknowledgments
This work was supported by the National Science Foundation under Grant No. 1562669, 1562821, and 1562490 as well as the Steel Diaphragm Innovation Initiative which is funded by the American Institute of Steel Construction, the American Iron and Steel Institute, the Steel Deck Institute, the Steel Joist Institute, and the Metal Building Manufacturers Association. Any opinions expressed in this paper are those of the authors alone, and do not necessarily reflect the views of the National Science Foundation or other sponsors.

References

AISC. (2016a). “Seismic provisions for structural steel buildings, (AISC 341-16)”. *American Iron and Steel Institute*. Chicago, IL: AISC.

AISC. (2016b). “Specification for structural steel buildings, (AISC 360-16)”. *American Iron and Steel Institute*. Chicago, IL: AISC.

ASCE. (2016). “Minimum design loads for buildings and other structures (ASCE standard)”, Reston, VA. *American Society of Civil Engineers*.

ASTM. (2019). Standard Specification for Carbon Structural Steel, (ASTM A36 / A36M-19). *ASTM International*, West Conshohocken, PA, 2019, www.astm.org

Avellaneda Ramirez, R.E., Easterling, W. S., Schafer, B.W., Hajjar, J.F., and Eatherton, M.R. (2019) “Cyclic Testing of Composite Concrete on Metal Deck Diaphragms Undergoing Diagonal Tension Cracking”, *12th Canadian Conference on Earthquake Engineering*, Chateau Frontenac, Quebec, QC.

Coffin, L.F. (1954). “A study of the effects of the cyclic thermal stresses on a ductile metal”, Translat. ASME, 76, 931-950.

Elkady, A. and D. G. Lignos. 2014. "Modeling of the Composite Action in Fully Restrained Beam-to-Column Connections: Implications in the Seismic Design and Collapse Capacity of Steel Special Moment Frames." *Earthquake Engineering and Structural Dynamics* 43 (13): 1935-1954. doi:10.1002/eqe.2430.

Farahi, M. and M. Mofid. 2013. "On the Quantification of Seismic Performance Factors of Chevron Knee Bracings, in Steel Structures." *Engineering Structures* 46: 155-164. doi:10.1016/j.engstruct.2012.06.026.

FEMA. (2009). Quantification of building seismic performance factors, (FEMA P695). Applied Technology Council, Federal Emergency Management Agency.

Kiggins, S., and Uang, C.-M. (2006). "Reducing Residual Drift of Buckling-Restrained Braced Frames as a Dual System", Engineering Structures, Vol. 28, pp. 1525-1532.

Koliou, M., Filiatrault, A., Kelly, D. J., Lawson, J.. (2016). "Buildings with Rigid Walls and Flexible Roof Diaphragms. I: Evaluation of Current U.S. Seismic Provisions." *Journal of Structural Engineering (United States)* 142 (3). doi:10.1061/(ASCE)ST.1943-541X.0001438.

Krawinkler (2000) "State of the Art Report on Systems Performance of Steel Moment Frames Subject to Earthquake Ground Shaking." Federal Emergency Management Agency, FEMA-355C, SAC Joint Venture.

Leng, J., Buonopane, S. G., & Schafer, B. W. (2020). Incremental dynamic analysis and FEMA P695 seismic performance evaluation of a cold-formed steel–framed building with gravity framing and architectural sheathing. *Earthquake Engineering & Structural Dynamics*, *49*(4), 394-412.

Malakoutian, M., J. W. Berman, P. Dusicka, and A. Lopes. 2015. "Quantification of Linked Column Frame Seismic Performance Factors for use in Seismic Design." *Journal of Earthquake Engineering*: 1-24. doi:10.1080/13632469.2015.1104750.

Manson, S.S. (1954). "Behaviour of Materials under Conditions of Thermal Stress", NACA TN-2933. *National Advisory Committee for Aeronautics*.

Martin, É. (2002). "Inelastic response of steel roof deck diaphragms under simulated dynamically applied seismic loading", Master's thesis, *Ecole Polytechnique de Montreal*.

Mazzoni, S., McKenna, F., Scott, M. H., & Fenves, G. L. (2006). OpenSees command language manual. *Pacific Earthquake Engineering Research (PEER) Center*, 264.

Newell J, Uang CM, Benzoni G. (2006). Subassemblage testing of core brace buckling restrained braces (G Series). University of California San Diego. Report no. TR2006/01; 2006.

Torabian, S., Eatherton, M.R., Easterling, W.S., Hajjar, J.F., Schafer, B.W. (2019). "SDII Building Archetype Design v2.0", *CFSRC Report R-2019-04*, jhir.library.jhu.edu/handle/1774.2/62106.

Wei, G., Eatherton, M.R., Foroughi, H., Torabian, S., and Schafer, B.W. (2020). Seismic Behavior of Steel BRBF Buildings Including Consideration of Diaphragm Inelasticity, Cold-Formed Steel Research Consortium Report Series, Report Number CFSRC R-2020-03. http://jhir.library.jhu.edu/handle/1774.2/62366

Zareian, F., Lignos, D. G., Krawinkler, H. (2010). "Evaluation of Seismic Collapse Performance of Steel Special Moment Resisting Frames using FEMA P695 (ATC-63) Methodology." ASCE Structures Congress 2010. doi:10.1061/41130(369)116.